Mathematical framework for a place code in the auditory system

Alex D. Reyes[1]

[1]Center for Neural Science, New York University, New York, NY, USA

Abstract

In the auditory system, tonotopy is postulated to be the substrate for a place code, where sound frequency is encoded by the location of the neurons that fire during the stimulus. Though conceptually simple, the computations that allow for the representation of intensity and complex sounds are poorly understood. Here, a mathematical framework is developed in order to define clearly the conditions that support a place code. The analyses suggest that the functional architecture of networks consists of overlapping neuron clusters whose size varies with intensity. Tone frequency and intensity are encoded, respectively, by the location and size of the activated clusters. Algebraic operations -addition and multiplication- are then derived to elucidate the rules for assembling and modulating multi-frequency sound in networks. Results of network simulations are consistent with the general predictions. This approach complements experimental and computational approaches and provides a mathematical foundation for interpreting data and constructing models.

Introduction

Many sensory systems are organized topographically so that adjacent neurons have small differences in the receptive fields. The result is that minute changes in the sensory features causes an incremental shift in the spatial distribution of active neurons. This is has led to the notion of a place code where the location of the active neurons provides information about sensory attributes. In the auditory system, the substrate for a place code is tonotopy, where the preferred frequency of each neuron varies systematically along one axis [1]. Tonotopy originates in the cochlea [2, 3] and is inherited by progressively higher order structures along the auditory pathway [4]. The importance of a place code [5] is underscored by the fact that cochlear implants, arguably the most successful brain-machine interface, enable deaf patients to discriminate tone pitch simply by delivering brief electrical pulses at points of the cochlea corresponding to specific frequencies [6].

Although frequency and intensity may be encoded in several ways [7], there are regimes where place-coding seems advantageous. Humans are able to discriminate small differences in frequencies and intensities even for stimuli as brief as 5-10 ms [8, 9, 10, 11]. Therefore, the major computations have already taken place within a few milliseconds. This is of some significance because in this short time interval, cortical neurons can fire only bursts of 1-2 action potentials [12, 13], indicating that neurons essentially function as binary units. Therefore, it seems unlikely that neither frequency nor intensity can be encoded via the firing rate of cells since the dynamic range would be severely limited. Similarly, coding schemes based on temporal or 'volley' schemes is difficult to implement at the level of cortex because neurons can phase-lock only to low frequency sounds [14, 15, 16].

There are, however, several challenges with implementing a place coding scheme. First, the optimal architecture for representing frequency is not well-defined. Possible functional units include individual neurons, cortical columns [17, 18], or overlapping clusters [19]. The dimension of each unit ultimately determines the range and resolution at which frequencies and intensities that can be represented and discriminated. Second, how both frequency and intensity can be encoded with a place code is unclear, particularly for brief stimuli when cells function mostly as binary units. Third, the rules for combining multiple stimuli is lacking. Physiological sounds are composed of pure tones with differing frequencies and intensities, resulting in potentially complex spatial activity patterns in networks. Finally, the role of inhibition in a place coding scheme has not been established.

Here, a mathematical model is developed in order to gain insights into: 1) the functional organization of the auditory system that supports a place coding scheme for frequency and intensity: and 2) the computations that can be performed in networks. The approach is to use principles from set theory and topology to construct the acoustic and neural spaces, find a mapping between the spaces, and then develop the algebraic operations. The predictions of the math model are then tested with simulations.

Results

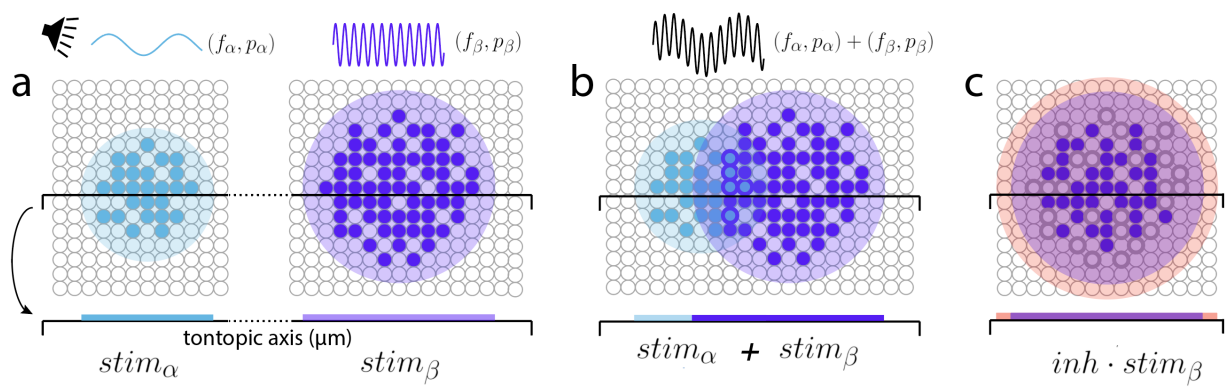

Figure 1: **Computations with a place code**. ***a, left***, hypothetical neural representation of a low frequency (f_α), small amplitude (p_α) pure tone stimulus in a two-dimensional neural network. A stimulus-evoked synaptic field covers a circular area (cyan disk) and causes a subset of cells to fire (filled circles). Projection of the synaptic field onto the tonotopic axis (cyan bar) gives the location and size of the activated area. ***right***, synaptic field generated by a tone with higher frequency (f_β) and sound pressure (p_β). ***b***, synaptic field generated by a sound composed of the two tones. ***c***, modulation by inhibition (red).

The mathematical model is subject to the following biological constraints. First, the neural network inherits the tonotopic organization of the cochlea [2, 3] so that the preferred frequency of neurons changes systematically with location along one axis. Second, a pure tone generates a synaptic field and activates a population of neurons within a confined area [20], with the location of the area varying with the tone frequency. Third, the area grows with sound intensity [20], paralleling the increase in the response area of the basilar membrane [21, 22]. The model is broadly related to the "spread-of-excitation" class of models [7, 23]

The basic computations that can be performed using a place code are shown schematically in a 2-dimensional network of neurons (Fig. 1). In response to a pure tone stimulus, a synaptic field is

generated within an enclosed area of the network (a, left panel, cyan disk), causing a population of cells to fire (filled circles). A tone with a higher frequency and intensity activates a larger area at a different location (right panel). A sound composed of the two pure tones activates both regions simultaneously; the regions may overlap if the difference in frequencies is small (Fig. 1b). Finally, excitatory synaptic fields and the activated neuron clusters are modulated by inhibition (Fig. 1c). The mathematical basis for these computations is developed below. For clarity, only the main results are shown (details in appendix).

Neural Space

Although the brain has three spatial dimensions, only one dimension -that corresponding to the tonotopic axis- is relevant for a place code. Thus, the circular synaptic field in Fig. 1 is projected onto the tonotopic axis (bars). For simplicity, the neural space is defined as a single row of neurons (Fig. 2a). In the presence of sound, afferents from an external source generates a synaptic field that covers a contiguous subset of neurons. In the following, a mathematical description of the neural space will be developed that accommodates the neural elements and synaptic fields.

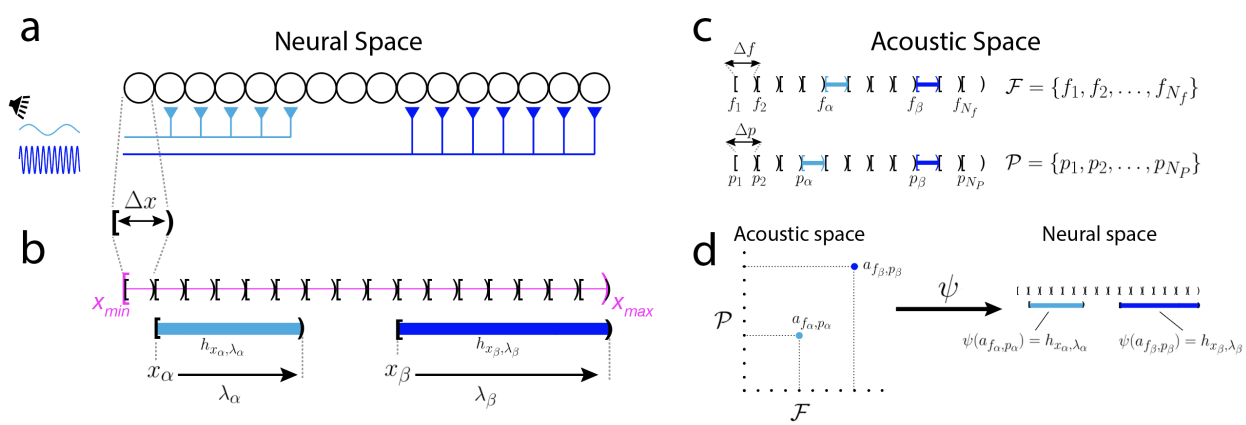

Figure 2: **Mathematical representation of neural and acoustic Spaces.** ***a***, neurons on the tonotopic axis are positioned next to each other with no space in between. Pure tone stimuli activate afferents onto a subset of neurons (cyan, blue). ***b***, mathematical representation of neural space. The tonotopic axis is a half-open interval (magenta) partitioned into smaller intervals that represent the space (Δx) taken up by neurons. The synaptic fields ($h_{x_\alpha,\lambda_\alpha}, h_{x_\beta,\lambda_\beta}$) are also half-open intervals. ***c***, The acoustic space has two dimensions, with frequency as one axis and pressure as the other. The frequency and pressure spaces are partitioned into half-open intervals of length $\Delta f, \Delta p$, respectively. ***d***, Mapping two tones in the acoustic space to intervals in neural space via a function ψ.

The neural space is defined as an interval, bounded by minimum and maximum values x_{min} and x_{max} (Fig. 2b, magenta). To incorporate neurons, the neural space is partitioned into N_{cell} sections. Both the neural space and the cells are 'half-open' intervals, which are closed ("[") on one end and open on the other (")"). This is convenient mathematically because neurons can be packed next to each other with no space in between, allowing for a formal definition of a partition (see appendix). Each neuron can therefore be expressed as non-overlapping subintervals of the form $[x, x + \Delta x)$, where Δx is the width of each neuron. Note that each neuron can be uniquely identified the point at the closed end, which also gives its location along the tonotopic axis. The set containing these points is:

$$\mathcal{X} = \{x_1, x_2, \ldots, x_{N_{cell}}\} \tag{1}$$

A synaptic field spans an integral number (n_λ) of neurons and is also a half-open interval with length $\lambda = n_\lambda \Delta x$. The length λ ranges from Δx (1 cell) to a maximum $\lambda_{max} = n_{max}\Delta x$. Each synaptic interval, designated as $h_{x,\lambda} = [x, x+\lambda)$, is uniquely identified by the location of the cell at the closed end (x_α, x_β in Fig. 2b) and by its length ($\lambda_\alpha, \lambda_\beta$). The set of starting points $\mathcal{X}_\lambda$ and the set of achievable lengths Λ are given by:

$$\begin{aligned} \mathcal{X}_\lambda &= \{x_1, x_2, \ldots, x_{N_\lambda}\} \\ \Lambda &= \{\lambda_1, \lambda_2, \ldots, \lambda_{max}\} \end{aligned} \tag{2}$$

As will be shown below, $\mathcal{X}_\lambda$ will contain information about the frequency while Λ will contain information about the sound pressure.

Mathematically, the set of all synaptic intervals in neural space is a basis for topology on the neural space, which will be used to define algebraic operations and construct mapping from acoustic space (see below, appendix).

Representing sound in neural space

The elements of acoustic space $\mathcal{A}$ are pure tones, each of which is characterized by a sine wave of a given frequency (f) and amplitude corresponding to sound pressure (p). Theoretically, frequencies and pressures can take an uncountable number of values but physiologically, the audible range is bounded by minimum and maximum values. In addition, the resolution is limited in that tones with small differences in frequencies or sound pressures cannot be discriminated (frequency and intensity difference limens [8, 9, 10, 11]).

The acoustic space therefore has two dimensions with frequency as one axis and sound pressure as the other. As was done for neural space, the frequency and pressure axes are defined as a half-open intervals and divided into non-overlapping subintervals expressed as $[f, f+\Delta f)$ and $[p, p+\Delta p)$, respectively (Fig. 2c). Physiologically, Δf and Δp may be viewed as the minimum frequency and pressure difference that can be discriminated. For example, two tones with frequencies f_α, f_β that are in the interval $[f_1, f_1 + \Delta f)$ will both be 'assigned' to f_1 (see appendix). Therefore, the sets of audible frequencies and pressures are given by the first points of each interval:

$$\begin{aligned} \mathcal{F} &= \{f_1, f_2, \ldots, f_{N_f}\} \\ \mathcal{P} &= \{p_1, p_2, \ldots, p_{N_p}\} \end{aligned} \tag{3}$$

Features of the acoustic space are represented in neural space via a mapping ψ (Fig. 2d; see appendix for formal treatment). A pure tone $a_{f,p}$ is mapped to an interval $h_{x,\lambda}$ by first mapping the components f to x and p to λ via $\psi_f(f) = x$ and $\psi_p(p) = \lambda$.

$$\psi(a_{f,p}) = h_{\psi_f(f), \psi_p(p)} = h_{x,\lambda} \tag{4}$$

By adjusting the number of elements in each space appropriately, the mapping becomes bijective (one-to-one, onto).

A mapping from acoustic space to intervals that are inhibitory can be similarly defined. The mapping is complicated by the fact that the number and receptive field properties of $\boldsymbol{E}$ and $\boldsymbol{I}$ cells differ. The mapping is under ongoing investigation but for purposes of the present analyses, the mapping is taken to be identical to that for $\boldsymbol{E}$.

Algebraic operations with synaptic intervals

Having formally described the mathematical structure of neural space, it is now possible to define the algebraic operations -addition and multiplication- for combining and modulating synaptic intervals (Fig.1b,c). An important condition that must be satisfied is that operations be 'closed'; that is, the result obtained with addition or multiplication is an interval (or intervals) that remains in neural space. To simplify notation, the intervals will henceforth be identified with a single subscript or superscript.

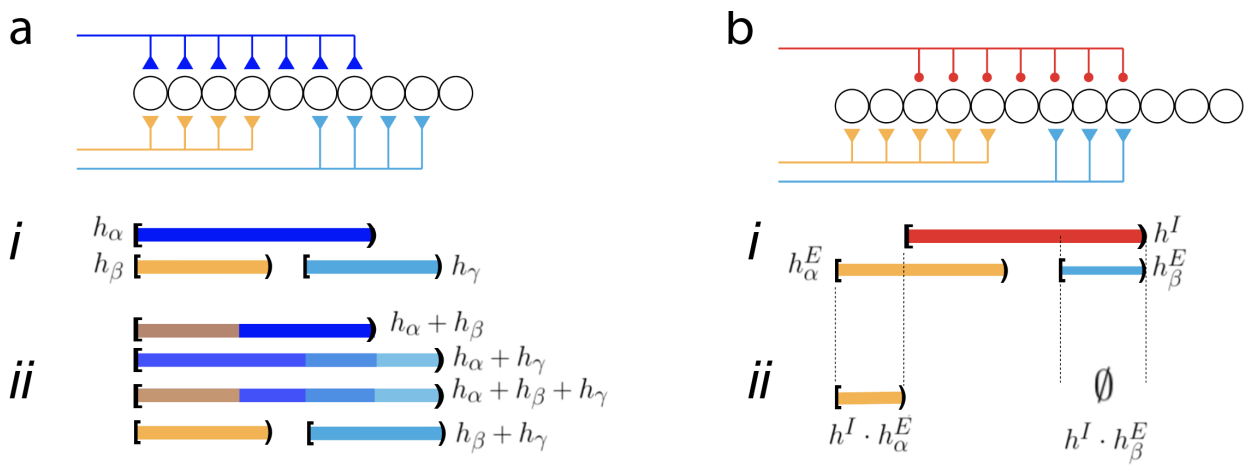

Figure 3: **Addition and Multiplication.** ***a***, schematic of network receiving three excitatory afferent inputs. ***i***, half-open intervals representing the synaptic fields. ***ii***, addition (union) of different combinations of intervals. **b**, schematic of network receiving two excitatory inputs (orange, cyan) and an inhibitory input (red). ***i***, half-open intervals associated with the activated afferents. ***ii***, multiplication (set minus) of each excitatory intervals by the inhibitory interval.

To satisfy closure, 'addition' of synaptic intervals is defined as their union. Let h_α, h_β be two synaptic intervals. Then,

$$h_\alpha + h_\beta \stackrel{\text{def}}{=} h_\alpha \cup h_\beta \tag{5}$$

The addition operation yields two possible results (see appendix for details). If the two synaptic intervals do not overlap (h_β, h_γ in Fig. 3ai), the union yields a set with the same two intervals (Fig. 3aii, bottom). If the two intervals overlap (h_α and h_β, h_α and h_γ), the result is a longer, single interval whose length depends on the amount of overlap (Fig. 3aii, top two traces). Note that if the starting points are the same (h_α and h_β), the length is equal to that of longer summand ($|h_\alpha + h_\beta| = |h_\alpha|, |h_\alpha| \geq |h_\beta|$), indicating that addition is sublinear.

It is noteworthy that there is some ambiguity from a decoding perspective because the addition operation will fuse overlapping intervals into a larger, single interval (e.g. $h_\alpha + h_\gamma$ in Fig. 3a). It would not be possible, for example, to determine whether a long synaptic interval is a result of a single high intensity pure tone, multiple pure tones with small differences in frequencies, or band limited noise.

Closure is satisfied because the union of an arbitrary number of overlapping intervals results in an interval that is always within the neural space. The union of any number of disjoint intervals is also within the neural space (more accurately, is a subset of the topology defined in neural space, see appendix). A notable property that will be important later is that there is no additive inverse that can decrease the interval length.

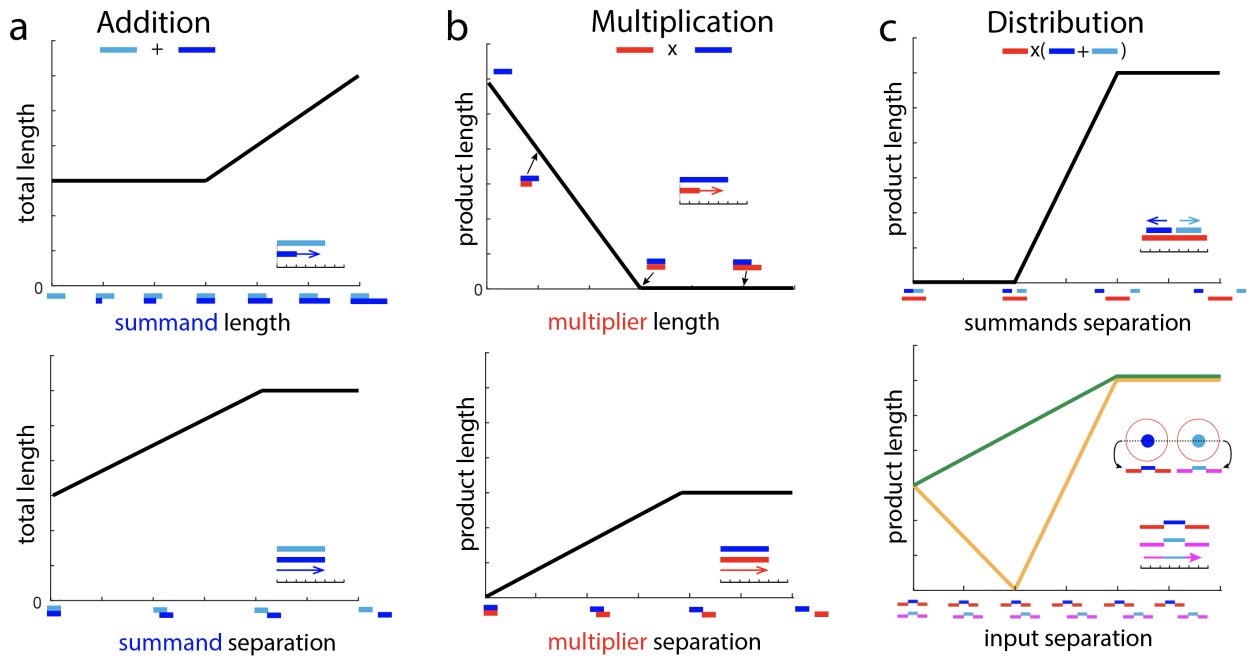

Figure 4: **Predicted effects of addition and multiplication**. ***a***, ***top***, addition of two intervals (cyan, blue) when the length of one interval (blue) is increased (top). ***bottom***, one interval (blue) is shifted to the right of the other (cyan). ***b*, top**, multiplication of an excitatory interval (blue) by an inhibitory interval of increasing length (red). ***bottom***, multiplication when the inhibitory interval is shifted to the right. ***c*, top**, effects of inhibition (red) on two excitatory intervals (blue, cyan). With the inhibitory interval at a fixed location, the distance between the excitatory intervals is increased systematically. ***bottom***, Effects of two inputs configured as center-surround where the excitatory intervals (blue, cyan) are each flanked by two inhibitory intervals (red, magenta). One of the inputs is shifted systematically to the right of the other. Predicted product length when the inputs occur simultaneously (orange) and when calculated with inputs delivered sequentially.

One example of addition that occurs under biological conditions is when a pure tone arrives simultaneously to the two ears. The signal propagates separately through the auditory pathway but eventually converges at some brain region. Because each input is due to the same tone, the resultant synaptic intervals will be at same location (i.e. have the same starting points) on the tonotopic axis, though their lengths may differ because of interaural intensity differences (orange and blue intervals in Fig. 3a). Fig. 4a (top panel) shows the predicted total length when two intervals with different lengths are added (the length of the cyan interval is fixed while that of the blue is increased). The total length is equal to the length of the longer interval: hence, it is initially constant and equal to that of the cyan interval but then increases linearly when the length of the blue interval becomes longer.

Addition also takes place when the sound is composed of two pure tones with different frequencies. This would generate two synaptic intervals with different starting points and possibly different

lengths (e.g. orange and cyan intervals in Fig. 3a). The total length depends on the degree of overlap between the intervals. In Fig. 4a (bottom panel), the location of one interval (cyan) is fixed while the other (blue) is shifted rightward. When the two intervals completely overlap, the total length is equal to the length of one interval. As the blue interval is shifted, the total length increases linearly and plateaus when the two intervals become disjoint.

Inhibition decreases the excitability of the network and would be expected to reduce the size of the synaptic interval. This is not possible with the addition operation because there is no inverse (i.e. 'subtraction' is not defined). Therefore, to incorporate the effects of inhibition, a 'multiplication' operation is introduced (Fig. 3b). Multiplication ('$\cdot$') of an excitatory synaptic interval h^E by an inhibitory interval h^I is defined as:

$$h^I \cdot h^E \stackrel{\text{def}}{=} h^E \setminus h^I \tag{6}$$

The set minus operation "$\setminus$" eliminates the points from the multiplicand h^E that it has in common with the multiplier h^I (Fig. 3b*i,ii*) thereby decreasing its length. Note that this differs from the usual set theoretic definition of multiplication, where the product of sets is given by their intersection. Multiplication yields several results, depending on the relative locations and size of the multiplicand and the multiplier (see appendix). If the $\boldsymbol{E}$ and $\boldsymbol{I}$ intervals do not overlap, then the $\boldsymbol{E}$ interval is unaffected. If the intervals overlap (h^E_α and h^I), then the $\boldsymbol{E}$ interval is shortened ($h^I \cdot h^E_\alpha$ in *ii*). If the $\boldsymbol{E}$ interval (h^E_β) is completely within the $\boldsymbol{I}$ interval, the product is the empty set, indicating complete cancellation ($h^I \cdot h^E_\beta$ in *ii*). Other possible outcomes are detailed in appendix.

Multiplication satisfies the closure property as the resulting interval is a half-open interval that is always in neural space. An important property is that multiplication is not commutative so that the order of operations matters: $h^I \cdot h^E \neq h^E \cdot h^I$. Other algebraic properties are discussed in appendix.

If the excitatory and inhibitory inputs are co-activated (as in feedforward circuits), then the $\boldsymbol{E}$ and $\boldsymbol{I}$ intervals will be at the same location (same starting points) on the tonotopic axis but may have different lengths. Fig. 4b (top panel) plots the predicted length of the product when the $\boldsymbol{E}$ interval is multiplied by $\boldsymbol{I}$ intervals of increasing lengths. The product length decreases and becomes zero when length of the $\boldsymbol{I}$ interval exceeds that of the $\boldsymbol{E}$ interval.

If the $\boldsymbol{E}$ and $\boldsymbol{I}$ inputs are independent of each other, the synaptic intervals could be at different locations on the tonotopic axis. Figure 4b (bottom panel) plots the length of the product when the starting point of the $\boldsymbol{I}$ interval (red) is shifted systematically to the right of the $\boldsymbol{E}$ interval (blue). The product length is zero when the $\boldsymbol{E}$ and $\boldsymbol{I}$ intervals overlap completely (separation = 0) and increases linearly as the overlap decreases, eventually plateauing to a constant value when the intervals become disjoint.

With addition and multiplication defined, the rules for combining the two operations can now be determined. A simple case is when a network receives two excitatory inputs that results in synaptic intervals (h^E_α, h^E_β) and a single inhibitory input that result in an inhibitory interval (h^I). This scenario would occur if binaural excitatory inputs that converge in a network are then acted on by local inhibitory neurons. When all three inputs are activated simultaneously, the intervals combine in neural space as $h^I \cdot (h^E_\alpha + h^E_\beta)$. It can be shown that multiplication is *left* distributive so that (see appendix):

$$h^I \cdot (h^E_\alpha + h^E_\beta) = (h^I \cdot h^E_\alpha) + (h^I \cdot h^E_\beta) \tag{7}$$

Intuitively, this means that the effect of a single inhibitory input on two separate excitatory inputs can be calculated by computing the inhibitory effects on each separately and then adding the results. Multiplication, however, is not *right* distributive. Thus, given two inhibitory intervals (h^I_α and h^I_β) acting on a single excitatory interval (h^E):

$$(h^I_\alpha + h^I_\beta) \cdot h^E \neq (h^I_\alpha \cdot h^E) + (h^I_\beta \cdot h^E) \tag{8}$$

Fig. 4 c (top panel) plots the predicted length when two $\boldsymbol{E}$ intervals are multiplied by an $\boldsymbol{I}$ interval as per eq. 7. The two $\boldsymbol{E}$ intervals (blue, cyan) are shifted left- and rightward relative to the $\boldsymbol{I}$ interval (red). The product length is zero as long as the two $\boldsymbol{E}$ intervals are within the $\boldsymbol{I}$ interval. When the two $\boldsymbol{E}$ intervals reach and exceed the borders of the $\boldsymbol{I}$ interval, the product length increases and reaches a plateau when the $\boldsymbol{E}$ and $\boldsymbol{I}$ intervals become disjoint.

A common physiological scenario is when sound is composed of two pure tones and each tone results in an excitatory synaptic field surrounded by an inhibitory field (center surround inhibition, Fig. 4c, bottom panel). The corresponding composite interval contains an excitatory interval that is flanked by two inhibitory intervals (inset). In Fig. 4c (bottom panel, orange curve), the location of one composite interval is shifted rightward. When the composite intervals coincide (separation =0), the product length is equal to that of a single excitatory interval. With increasing separation, the product length decreases towards zero but then increases, reaching a plateau when the excitatory and inhibitory components of each composite interval no longer overlap.

Letting the $\boldsymbol{E}$ -$\boldsymbol{I}$ interval pair for one tone be h^E_α, h^I_α and that for the other tone be h^E_β, h^I_β, the mathematical expression describing the computation is:

$$(h^I_\alpha + h^I_\beta) \cdot (h^E_\alpha + h^E_\beta) \tag{9}$$

An important consequence of the distributive properties of multiplication is that eq. 9 is generally not equivalent to multiplying each excitatory interval by its associated interval first and then adding the results:

$$(h^I_\alpha + h^I_\beta) \cdot (h^E_\alpha + h^E_\beta) \neq (h^I_\alpha \cdot h^E_\alpha) + (h^I_\beta \cdot h^E_\beta) \tag{10}$$

The green curve in Fig. 4 c (bottom panel) is the predicted product length when the $\boldsymbol{E}$ -$\boldsymbol{I}$ pair are delivered separately and their product lengths subsequently summed.

Simulations with spiking neurons

Key features of the mathematical model were examined with simulations performed on a 2 dimensional network model of spiking excitatory and inhibitory neurons [24]. Both $\boldsymbol{E}$ and $\boldsymbol{I}$ neuron population receive a Gaussian distributed excitatory drive from an external source (Fig. 5a); the $\boldsymbol{E}$ cells in addition receive feedforward inhibitory inputs from the $\boldsymbol{I}$ cells. Stimulation evokes Gaussian distributed excitatory inward currents in both populations and also inhibitory currents in the $\boldsymbol{E}$ cells (profiles of currents shown in insets). With brief stimuli, the recurrent connections between neurons [25] did not contribute significantly to activity in auditory cortical circuits [24] and were omitted. The region encompassing neurons that fire is henceforth referred to as the activated area (Fig. 5b, top panel). The underlying synaptic field (bottom panel) is defined as the area of the network where the *net* synaptic inputs to cells exceeded (were more negative than) rheobase, the minimum current needed to evoke an action potential (I_{Rh}, inset). As defined, the synaptic field

is a composite of all the inputs, both excitatory and inhibitory, that are evoked during a stimulus. Both the activated area and the synaptic field are quantified either by the diameters of circles fitted to the boundary points (magenta) or by the length of their projections to one axis (orange bar). Note that the spatial dimensions have units of *cell number* (see Methods to convert to microns).

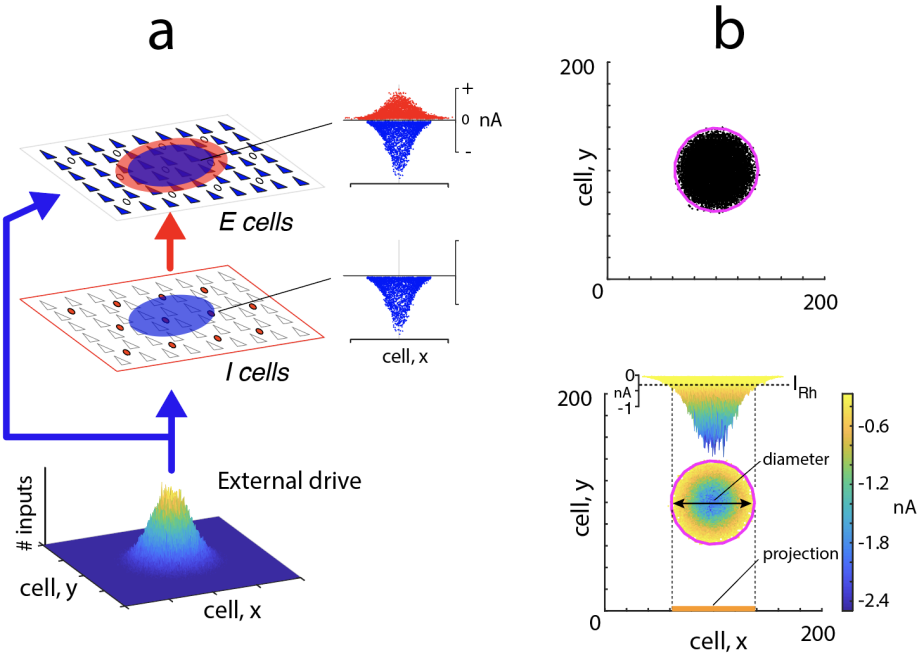

Figure 5: **Simulations with spiking neurons.** ***a***, Network consists of excitatory and inhibitory neuron populations. An external drive evokes excitatory inputs in both populations (blue disks) and inhibitory inputs to the ***E*** cells (red disk). ***insets***, profiles of excitatory (blue) and inhibitory (red) currents evoked in the ***E*** and ***I*** populations. ***b, bottom***, synaptic field evoked in the network during a stimulus. The spatial extent of the synaptic field is quantified either by the diameter of a circle fitted to its outermost points (magenta) or by the length of its projection to the tonotopic axis (orange bar). ***inset***, profile of net synaptic current generated in the ***E*** cell population. The perimeter of the synaptic field encompasses cells whose net synaptic current input exceeded rheobase (I_{Rh}). ***top***, activated area contains cells that fired action potentials (dots).

To test the addition operation, two external excitatory drives were delivered to the center of the network simultaneously (without inhibition). Increasing the width (by increasing the standard deviation σ_α of the external drive) of one stimulus, while keeping that (σ_β) of the other fixed, increased the diameters of the synaptic field and activated areas (Fig. 6a, top panel, *i-iii*). As predicted, the diameters of the synaptic field (bottom panel, orange) and activated area (black) initially did not change when σ_α was smaller than σ_β ($\frac{\sigma_\alpha}{\sigma_\beta} < 0.5$) but then increased as σ_α continued to widen. However, because the synaptic currents were Gaussian distributed (Fig. 5b, bottom panel), the curve started to increase before σ_α became equal to σ_β ($\frac{\sigma_\alpha}{\sigma_\beta} = 1$). When delivered simultaneously, the magnitude of the composite current increased, causing the region that exceeded rheobase to widen (Fig 6 a, top panel, compare synaptic field evoked with a single stimulus (*i*) to that evoked with 2 stimuli (*ii*)). The diameter can be calculated from the standard deviations of the two inputs (diameter $\propto \sqrt{\sigma_\alpha^2 + \sigma_\beta^2}$, not shown).

To examine the addition of spatially disparate synaptic fields, two excitatory inputs were deliv-

ered at different distances from each other (Fig. 6b, top panel). Consistent with the prediction, the projection lengths of the synaptic field (bottom panel, orange) and activated areas (black) increased with stimulus separation and reached a plateau when the two inputs became disjoint (*iii*). The projection lengths were greater than predicted (dashed lines) when the separation was small (< 10 cells) and when the intervals were just becoming disjoint (at separation ~ 40 cells, *ii*) due to the summation properties of the Gaussian distributed inputs discussed above.

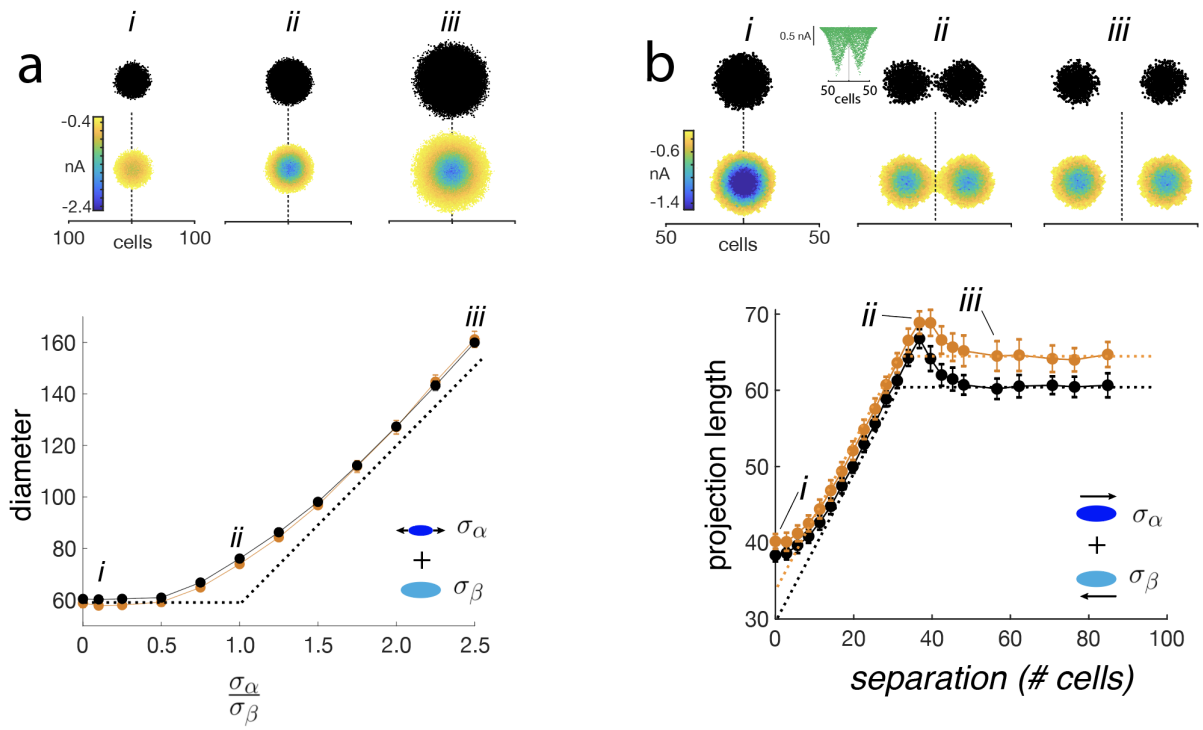

Figure 6: **Test of addition.** ***a, top***, Activated area (top; 1 sweep) and underlying synaptic field (bottom; average of 25 sweeps). ***i***, one stimulus. ***ii-iii***, two stimuli delivered to the center of the network. The width of one input was systematically increased (σ_α: 2- 45 cells) while that of the other ($\sigma_\beta = 20$ cells) was kept constant. ***bottom***, plot of synaptic field (orange) and activated area (black) diameters vs $\frac{\sigma_\alpha}{\sigma_\beta}$. Dashed curve is predicted relation. ***b***, addition of two spatially separated excitatory inputs ($\sigma_\alpha = \sigma_\beta = 10$). ***top, i - iii***, activated areas and synaptic fields with increasing stimulus separation. Inset in ***ii*** shows example of excitatory synaptic current profiles. ***bottom***, projection length vs. separation distance for synaptic field (orange) and activated area (black). Dashed curves are predicted changes.

To test the multiplication operation, the ***E*** and ***I*** neurons were stimulated simultaneously, resulting in excitatory and inhibitory synaptic currents in the ***E*** cells (inset in top panel of Fig. 7a *ii*). The width of the excitatory input (σ_{exc}) was kept constant while that of the inhibitory input (σ_{inh}) was increased systematically. As predicted, the diameter of the synaptic field (bottom panel, orange) and activated area (black) decreased with increasing σ_{inh}. However, the diameter asymptoted towards a non-zero value. Because the network was feedforward, the inhibitory input was delayed relative to excitation by about 10-15 ms; as a result, there was always a time window where excitation dominated. The excitatory synaptic input was not canceled even when the inhibition was twice as wide (top panel, *iii*).

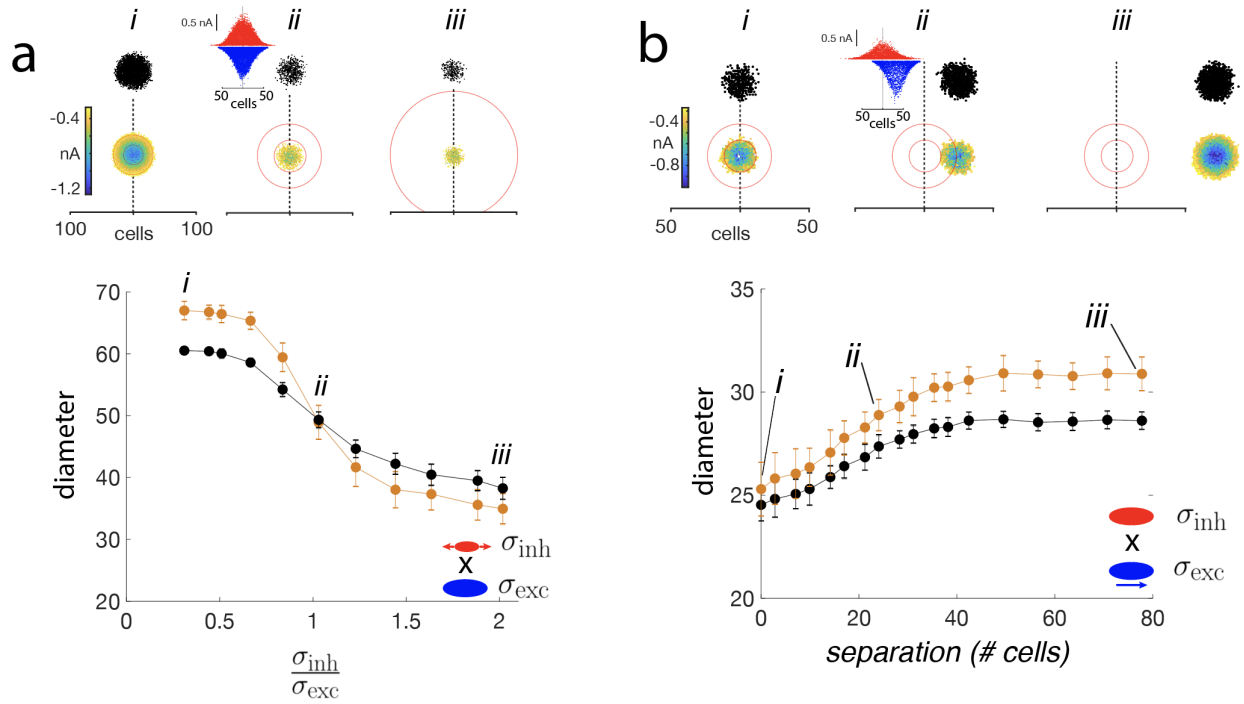

Figure 7: **Test of multiplication.** ***a, top, i-iii*** activated areas and synaptic fields evoked with excitatory ($\sigma_{exc} = 20$) and inhibitory ($\sigma_{inh} = 2 - 45$) inputs. The spatial extent of the inhibition is demarcated by the red circles (inner circle: 1 σ_{inh}; outer: 2 σ_{inh}). Inset in ***ii*** shows an example of excitatory (blue) and inhibitory (red) synaptic current profiles. ***bottom***, plot of activated area (black) and synaptic field (orange) vs $\frac{\sigma_{inh}}{\sigma_{exc}}$. ***b***, Same as in ***a*** except that the excitatory input ($\sigma_{exc} = 10$) was shifted systematically to the right of inhibition ($\sigma_{inh} = 10$). ***bottom***, Diameters of activated area (black) and synaptic field (orange) plotted against separation between excitatory and inhibitory synaptic fields

.

To examine multiplication of spatially disparate ***E*** and ***I*** inputs, the excitatory input was shifted systematically to the right of the inhibitory input (Fig. 7b). As predicted, the diameters of the synaptic field (bottom panel, orange) and activated area (black) increased with the ***E*** -***I*** separation and plateaued when the ***E*** and ***I*** inputs became disjoint (*iii*).

To examine how multiplication distributes over addition, two excitatory inputs and one inhibitory input were delivered simultaneously to the network (Fig. 8a). This is the analog of the left hand side of (eq. 7). All three inputs were initially at the center and then with the inhibition stationary, the two excitatory inputs were shifted left and right (Fig. 8a, top panel, *i-iii*). As predicted, the projection length of the synaptic field increased towards an asymptotic value (bottom panel, orange). To reproduce the right hand side of eq. 7, simulations were performed with inhibition, first with one of the excitatory inputs and then with the other; the resultant projection lengths of each were then summed (green). As was observed with simultaneous stimulation, the projection length increased with separation. The match was poor at small separations <10 cells (*i*) and at separation of $\sim$ 30 cells (*ii*) because the interaction between the Gaussian excitatory currents (see above) did not factor in when each input was delivered separately. The two curves were nearly identical at separations of 40-80 cells. In this range the ***E*** inputs were disjoint (as indicated by the plateauing of the excitation-only curve (dashed orange)) but still overlapped with

the inhibitory synaptic field (the orange and green curves were below the excitation-only curve).

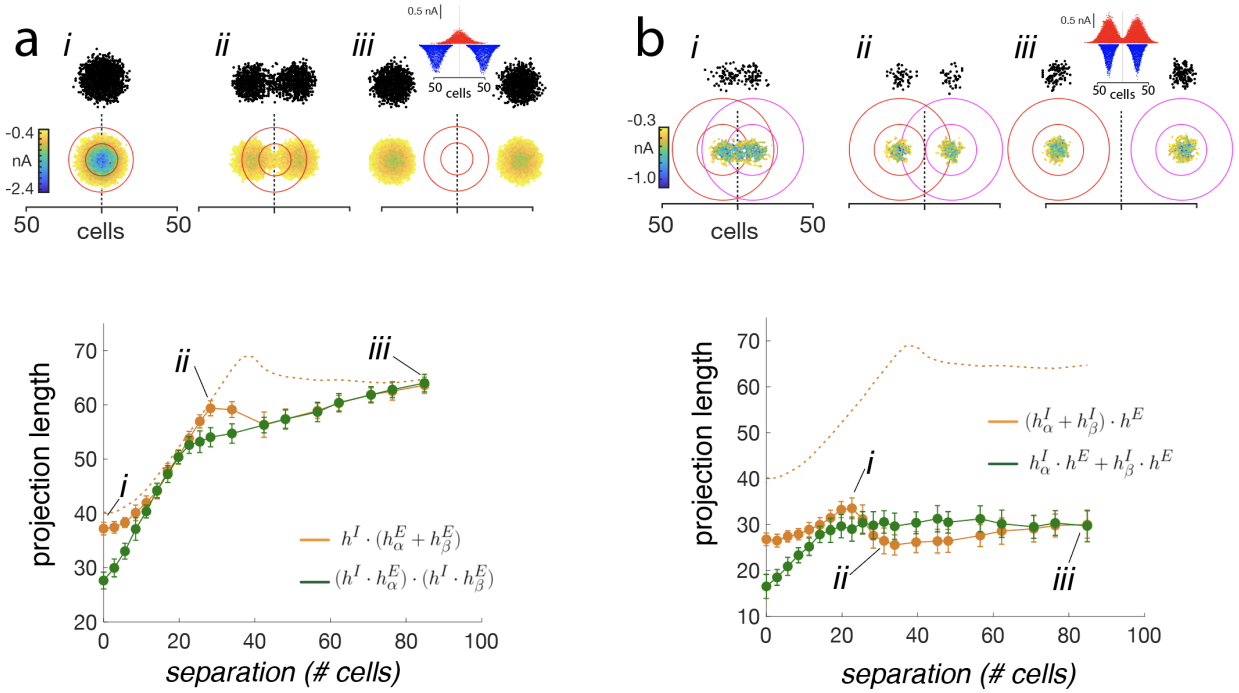

Figure 8: **Test of distributive properties.** ***a, top, i-iii*** Representative activated areas and synaptic fields generated by two excitatory inputs and a single inhibitory input ($\sigma_{exc} = \sigma_{inh} = 10$). With the location of inhibition fixed, the two excitatory inputs were separated systematically. The spatial extent of the inhibition is demarcated by the red circles (inner circle: 1 σ_{inh}; outer: 2 σ_{inh}). Inset in ***iii*** shows the excitatory (blue) and inhibitory (red) synaptic current profiles. ***bottom***, plot of synaptic field projection lengths (orange) vs separation of the excitatory inputs. Green symbols are projection lengths obtained with the sequential stimulation protocol (see text). Dotted curve is with no inhibition. ***b***, Simulations with two excitatory-inhibitory pairs, each with center-surround configuration (see inset in ***iii***). ***bottom***, legend as in ***a*** except that the green traces plot the projected lengths obtained when each ***E*** - ***I*** pair ($\sigma_{exc} = 10, \sigma_{inh} = 17$) was delivered sequentially (see text).

Finally, the interaction of inputs with center-surround inhibition (eq. 9) was examined by delivering two excitatory inputs, each with associated inhibitory components (inset in Fig, 8b, top panel, *iii*), to the network. The distance between the inputs were then increased systematically and the projection lengths measured (bottom panel, orange curve). At separations > 20 cells, the projection length of the synaptic field decreased to a minimum (*ii*) and then increased towards a plateau (*iii*), consistent with the prediction (Fig. 4c, bottom panel). However, at separations < 20 cells, the length increased instead of decreasing; this is likely due to the interaction of the Gaussian distributed excitatory fields discussed above. To confirm that the same result cannot be obtained by presenting each stimulus separately (right hand side of eq. 10), each ***E*** -***I*** pair was delivered sequentially and the individual projection lengths summed. Unlike with simultaneous stimulation and consistent with the prediction (green curve in Fig. 4c,bottom panel), the projection length increased monotonically to a plateau without a dip (green curve).

Discussion

The aim of this study was to develop a mathematical framework for a place-code and derive the underlying principles for how tones of varying frequencies and intensities are represented, assembled, and modulated in networks of excitatory and inhibitory neurons. The model is not intended to replicate the detailed dynamics of biological networks but rather to provide a 'skeleton' to aid in the interpretation of experimental data and the construction of biologically-inspired computer simulations.

Key findings are as follows (detailed below). First, the 'functional unit' of neural space is a set of contiguous neurons that have flexible borders. The associated mathematical architecture, or topology, is a collection of half-open intervals of varying lengths. The frequency and intensity of pure tones are encoded solely by the location and length of the intervals. Second, the architecture dictated the range and resolution of tone frequencies and intensities that can be represented in neural space. Finally, computations in neural space for combining and modulating units are 'addition' defined as the union and 'multiplication' defined as the set minus operation. The associated algebraic laws limit the type of computations that can be performed on the intervals.

Significance and Implications

In order to encode both frequency and intensity, the 'functional' units in the model have flexible borders that can expand, unlike classical cortical columns [17]. Each is a contiguous set of neurons that receive tone-evoked synaptic inputs (synaptic field). Encoding sound involves mapping a point in acoustic space (pure tone with frequency f and pressure p) to an element in neural space (interval at location x with length λ). Other variables such as firing rate, spike timing, or response patterns are not essential but may play a more complementary roles. Frequency and intensity discrimination, for example, improves with stimulus duration [8, 9, 10, 11]. It is noteworthy that a tone is represented by a population of neurons and it is not possible to decode the tone frequency or intensity from the firing of a single neuron.

The algebraic operations determine the computations that can be performed with a place code. An important property for addition and multiplication is that the results remain within the neural space (closure property). This would not be true, for example, if addition is defined as the standard sum of the interval lengths ($|h_\alpha|+|h_\beta|$) because the result could exceed the boundaries of the neural space if each interval is too long or located near the edge of the tonotopic axis. Similarly, defining the effect of inhibition as subtraction ($|h^E|-|h^I|$) could produce negative intervals. These difficulties were avoided by defining addition as the union and multiplication as the set difference operation. Compared with the more familiar vector space, the number of allowable computations is relatively limited (see appendix); many of the linear algebraic operations used commonly for analyses and computational models are not permitted.

One prediction is that adding two overlapping intervals with the starting points will result in an interval with length equal to that of the longer summand (i.e. $|h_\alpha|+|h_\beta| = |h_\alpha|$, $|h_\alpha| \geq |h_\beta|$). There is some experimental evidence in the inferior colliculus where the response evoked with binaural stimulation is equal to the larger of the two responses evoked with stimulation of either ear [26] (see figure in appendix). A possible psychophysical analog is that a tone presented binaurally is perceived to be less than twice as loud as monaural stimulation [27]. In both examples, the apparent sublinear effects arises from the properties of addition operation, and may not necessarily involve inhibitory processes.

The distributive properties suggest how multiple excitatory inputs can be modulated by multiple inhibitory inputs. The effect of inhibition acting on two excitatory inputs (e.g. modulation of

convergent binaural inputs by local inhibitory interneurons) can be predicted by examining the effects of inhibition on each input separately and then summing the results (eq. 7). However, this is not true for two sources of inhibition acting on a single excitatory interval (eq. 8). In cortical circuits, for example, excitatory neurons can be innervated by several classes of inhibitory interneurons [28]. In this case, the model suggests that accurately determining the overall effect of inhibition requires that the inhibitory interneurons be stimulated simultaneously; estimating the effect by sequential stimulation of each inhibitory inputs is generally incorrect.

The model shows that an inherent problem with the place coding scheme is that it is not possible to completely decode features of multi-component sound stimulus. Although the mapping from acoustic space to neural space is bijective, some ambiguities arise when a sound consists of tones with similar frequencies and/or high intensities. In neural space, the intervals are more likely to fuse into fewer intervals. Mathematically, the addition operation is a mapping from a two dimensional space to a one dimensional space (see appendix). The problem is akin to finding the combination of integers that sum to 10. The ambiguity is manifested in psychophysical experiments: subjects perceive tones with small differences in frequencies as a single, louder tone [29] and have difficulties distinguishing the individual components of a multi-frequency stimulus [30, 31].

Although the model was developed for networks, it may apply generally to other aspects of auditory neuroscience. A well-documented phenomenon in auditory psychophysics is that perceived loudness of two tones presented simultaneously does not increase until the frequency difference exceeds a 'critical band' [32, 33]. Assuming that loudness perception is related to the length of synaptic interval, this phenomenon may be expressed mathematically as $h_\alpha + h_\beta + h_{CB}$, where h_α, h_β represent the intervals generated by two tones and h_{CB} is the 'interval' of the critical band. Hence, $|h_\alpha + h_\beta + h_{CB}| = |h_\alpha \cup h_\beta \cup h_{CB}| = |h_{CB}|$ if $h_\alpha, h_\beta \subset h_{CB}$ but starts increasing when either intervals fall outside the critical band, much like Fig. 4a (top panel).

Finally, the mathematical architecture sets up the rules for transmitting information across brain regions. With the topologies and algebraic structures of neural networks known, it is possible with standard mathematical techniques to determine whether the mapping between neural spaces is e.g. continuous and bijective and whether the operations are preserved. Conversely, it is also possible to determine the optimal topology of the target or recipient space that would produce a desired mapping. In this study, for example, the structure of the acoustic space needed to create a bijective, continuous mapping to neural space was derived from the topology of the neural space.

Assumptions and limitations

The mathematical model is based on two salient features of the auditory system. One is that the neural space is organized tonotopically. Tonotopy has been described in most neural structures in the auditory pathway, from brainstem areas [4, 34, 35] to at least layer 4 of primary auditory cortex. Whether tonotopy is maintained throughout cortical layers is controversial, with some studies (all in mice) showing clear tonotopy [36, 37, 38, 39] and others showing a more 'salt-and-pepper' organization [40, 41, 39]. A salt-and-pepper organization suggests that the incoming afferents are distributed widely in the neural space rather than confined to a small area. The model needs a relatively prominent tonotopy to satisfy the requirement that synaptic intervals encompass a contiguous set of cells.

A second requirement is that the size of the synaptic interval and activated area increase with the intensity of the sound. Intensity-related expansion of response areas occurs in the cochlea [21, 22, 42] and can also be inferred from the excitatory frequency-response areas (FRAs) of individual neurons. The FRAs, which document the firing of cells to tones of varying frequencies and intensities, are typically "V-shaped". At low intensities, neurons fire only when the tone frequencies are

near its preferred frequency (tip of the V). At higher intensities, the range of frequencies that evoke firing increases substantially [43, 37]. If adjacent neurons have comparably-shaped FRAs but have slightly different preferred frequencies, an increase in intensity would translate to an increase in the spatial extent of activated neurons.

The algebraic operations were derived from set theoretic operations and the magnitude of the underlying synaptic inputs were irrelevant. Under biological conditions, the input magnitude determines the degree to which biophysical, synaptic, and network processes become engaged and will affect the length of the synaptic intervals and activated areas. Not surprisingly, the results of the network simulations deviated quantitatively from the mathematical predictions in some regimes (compare Fig. 4 to Figs 6, 7). Most of the discrepancies in the simulations were because the magnitudes of the synaptic inputs were Gaussian distributed along the tonotopic axis. In biological networks, the discrepancies may be exacerbated by the presence of threshold processes such as regenerative events [44, 45]. Though the algebraic operations remain valid overall, they may be obscured in regimes such as these.

The model incorrectly assumes that the strength of inhibition is sufficiently strong to fully cancel excitation. This facilitated analysis because the effect of multiplication depends solely on the overlap between the multiplicand and multiplier. As the simulations with the feedforward network showed, the excitation cannot be fully canceled by inhibition owing to synaptic delay. Moreover, the balance may be spatially non-homogeneous: in center-surround suppression, excitation dominates at the preferred frequency with inhibition becoming more prominent at non-preferred frequencies [43, 46, 47]. To apply multiplication to biological systems, it may be necessary to define empirically an "effective" inhibitory field that takes into account for $\boldsymbol{E}$ -$\boldsymbol{I}$ imbalances.

Relation to experiments

The functional unit was defined as the synaptic interval rather than the activated area, which reflects the number of neurons that actually fired. This facilitated analyses because multiplication by inhibitory synaptic intervals could be more easily incorporated into the mathematical framework. Though measuring the intracellular potentials of a large population of cells is currently not feasible experimentally, the extent of the synaptic field may be estimated from the activated area (Figs. 5,6,7,8), which can be measured with imaging techniques. Also, as mentioned above, the size of the synaptic field can also be indirectly inferred from the receptive fields of individual neurons.

For mathematical convenience, the location of the synaptic intervals was identified by the leftmost point (closed end) of the interval with increases in intensity signaled by a lengthening of the interval in the rightward (high frequency) direction. Similar behavior has been observed in the cochlea albeit in the opposite direction: an increase in the intensity causes response area to increase towards low frequency region of the basilar membrane while the high frequency cutoff remains fixed [42, 22, 3]. The choice of the leftmost point to tag the interval is arbitrary and any point in the interval will suffice provided an analogous point can be identified uniquely in each interval in the set. Experimentally, using the center of mass of active neurons as the identifier might be more practical.

Alternatives to interval-based place code

As discussed above, a shortcoming of the interval-based place code is the fusion of intervals that can occur when the sound has multiple tonal components, leading to ambiguities in decoding. In principle, this problem may be mitigated by re-defining the neural space so that the functional elements are non-overlapping clusters of neurons, similar to the classical cortical column [17] (see

appendix). For this model, frequency is encoded by the location of the columns and sound pressure by the number of neurons that fire within a column (the stimulus is assumed brief so that neurons are binary units). The result is that the units remain separate regardless of the number or intensity of the tonal components. A major disadvantage, however, is that it is difficult to encode a large frequency range without compromising the number of pressure levels that can be represented. To maximize the frequency range, the number of columns should be large, which means that the column size should be as small as possible. In contrast, to maximize the number of pressure levels, the column size should be as large as possible so as to contain more cells (see appendix).

Another alternative is a purely combinatorial code [48, 49], where coding sound features is based on which combination of neurons are activated, without reference to their location or rate. The main advantage is that the number of possible features (for binary neurons) that can represented is potentially very large (2^n, n = number of neurons). Ambiguities in representing multiple tones could be conceivably be avoided if there many neurons. However, this means that the 'look-up' table for decoding all the possible combinations of activity patterns is also very large. Moreover, without some organizing principle, it may be more difficult to define mappings between different brain regions.

Methods and Materials

Simulations were performed with a modified version of a network model used previously [24]. Briefly, the model is a 200 x 200 cell network composed of 75% excitatory ($\boldsymbol{E}$) and 25% inhibitory ($\boldsymbol{I}$) neurons. The connection architecture, synaptic amplitudes/dynamics, and intrinsic properties of neurons were based on experimental data obtained from paired whole-cell recordings of excitatory pyramidal neurons and inhibitory fast-spiking and low threshold spiking interneurons [25]. For this study, the low-threshold spiking interneurons and the recurrent connections between the different cell types were removed, leaving only the inhibitory connections from fast spiking interneurons to pyramidal neurons. The connection probability between the inhibitory fast-spiking cells and the excitatory pyramidal cells was Gaussian distributed with a standard deviation of 75 μm and peak of 0.4 [25].

Both $\boldsymbol{E}$ and $\boldsymbol{I}$ cells received excitatory synaptic barrages from an external source. The synaptic barrages to each cell (50 ms duration) represented the activity of a specified number of presynaptic neurons; the number was Gaussian distributed in space (Fig. 5 a, bottom). This resulted in excitatory synaptic currents in the $\boldsymbol{E}$ and $\boldsymbol{I}$ cell populations and inhibitory synaptic currents in the $\boldsymbol{E}$ cell population after the $\boldsymbol{I}$ cells fired (insets in Fig. 5a). The spatial extents of the synaptic inputs were varied by changing the standard deviations of the external drive. In some simulations, the $\boldsymbol{E}$ and $\boldsymbol{I}$ cell populations were uncoupled and received separate inputs that could be varied independently of each other.

The neurons are adaptive exponential integrate-and-fire units with parameters adjusted to replicate pyramidal and fast spiking inhibitory neuron firing (see [24] for the parameter values). The cells fired at most one action potential when stimulated with the synaptic barrage. The synaptic barrages were randomized so that the synaptic fields and activated areas varied from trial to trial.

The synaptic field was defined as the area of the network where the net synaptic currents to the cells exceeded rheobase, the minimum current needed to evoke an action potential in the $\boldsymbol{E}$ cells (I_{Rh}, inset in Fig. 5b, bottom panel). I_{Rh} was estimated by calculating the net synaptic current near firing threshold (V_θ): $I_{\text{net}} = g_{exc} * (V_\theta - E_{exc}) + g_{inh} * (V_\theta - E_{inh})$ where g_{exc}, g_{inh} are the excitatory and inhibitory conductances, respectively, and $E_{exc} = 0$ mV, $E_{inh} = -80$ mV are the reversal potentials. For the $\boldsymbol{E}$ cells, rheobase is approximately -0.27 nA.

The spatial extent of the synaptic field or activated area was quantified as the diameter of a circle fitted to the outermost points (maroon circles in Fig. 5b). In simulations with multiple components, the spatial extents were quantified as the total length of the projection onto the tonotopic axis (orange bar in Fig. 5b, bottom panel). The diameters and lengths have units of cell number but can be converted to microns by multiplying by 7.5 μm, the distance between $\boldsymbol{E}$ cells in the network. For all plots, the data points are plotted as mean +/- standard deviation compiled from 20-100 sweeps.

Acknowledgements

I thank L-S Young and A. Bose for reading the manuscript and providing helpful comments. This work was supported by DARPA- Lifelong Learning Machines

Appendix

Acoustic Space

The general approach for defining acoustic space is as follows. The elements of acoustic space are pure tones of varying frequencies and sound pressures. It is therefore a product of frequency space $S_{\mathcal{F}}$ and pressure space $S_{\mathcal{P}}$: $S_{\mathcal{A}} = S_{\mathcal{F}} \times S_{\mathcal{P}}$. Biologically, the range of audible and discriminable frequencies and sound pressures are limited. To reflect this, the frequency and pressure spaces will each be defined as a topological space where the underlying set is an interval but the topology is coarser than the usual topology.

The frequency space ($S_{\mathcal{F}}$) is defined as a half-open interval on the positive real line: $S_F = [f_{min}, f_{max}) \subset \mathbb{R}^+$, where f_{min}, f_{max} are the minimum and maximum audible frequencies, respectively. To account for the fact that discriminability is limited (i.e. tones of similar frequencies are perceived as the same), $S_{\mathcal{F}}$ is partitioned into N_f half-open intervals $h_f = [f_\alpha, f_\beta) = [f_\alpha, f_\alpha + \Delta f)$ where $\Delta f = \frac{1}{N_f}$ is the length of the interval and represents the minimum frequency difference that can be discriminated. The use of half-open intervals ensures that there is no 'gap' between adjacent frequency intervals. The set of all half-open intervals is:

$$\begin{aligned} \mathcal{H}_{\mathcal{F}} &= \{h_{f_i} = [f_i, f_i + \Delta f), f_i \in S_{\mathcal{F}}, f_i \leq |S_{\mathcal{F}}| - \Delta f\} \\ &= \{h_f = [f_{min} + i\Delta f, f_{min} + (i+1)\Delta f) \mid i \in \mathbb{N}_0, i < N_f\} \end{aligned} \tag{1}$$

The topology $\tau_{\mathcal{F}}$ is generated by the elements of $\mathcal{H}_f$:

$$\tau_{\mathcal{F}} = \{\bigcup H_f \mid H_f \subseteq \mathcal{H}_{\mathcal{F}}\} \tag{2}$$

The set of intervals is a partition where each interval is an equivalence class $[f_j]$: for $f_\alpha, f_\beta \in S_F, f_\alpha \sim f_\beta$ if $f_\alpha, f_\beta \in [f_i, f_i + \Delta f)$. This may be extended so that $f_\alpha \sim f_\beta$ if $f_\alpha, f_\beta > f_{max}$ and $f_\alpha \sim f_\beta$ if $f_\alpha, f_\beta \leq f_{min}$. Frequencies f_α, f_β are 'assigned' to f_i if they are between f_i and $f_i + \Delta f$. Thus, f_α, f_β are indistinguishable from each other since both are classified as f_i. Each frequency interval is uniquely identified by the minimum point at the closed end. The set of these points is:

$$\begin{aligned} \mathcal{F} &= \{f_i \mid f_i = f_{min} + i\Delta f, i \in \mathbb{N}_0, i < N_f\} \subset S_{\mathcal{F}} \\ &= \{f_0, f_1, \ldots, f_{N_f - 1}\} \end{aligned} \tag{3}$$

$\mathcal{F}$ is a discretization of $S_{\mathcal{F}}$ and may be thought of as a set of audible frequencies.

The sound pressure space is constructed similarly to yield:

$$\begin{aligned} &a. \quad \mathcal{P} = \{p_1, p_2, \ldots, p_{N_P}\} \subset S_{\mathcal{P}} \text{ (set of audible pressures)} \\ &b. \quad \mathcal{H}_{\mathcal{P}} = \{h_p \mid h_p = [p, p + \Delta p) \mid p \in \mathcal{P}\} \text{ (set of half open intervals)} \\ &c. \quad \tau_{\mathcal{P}} = \{\bigcup H_p \mid H_p \subseteq \mathcal{H}_{\mathcal{P}}\} \text{ (topology of } S_{\mathcal{P}}) \end{aligned} \tag{4}$$

The basis for a topology in $\mathcal{A} = S_{\mathcal{F}} \times S_{\mathcal{P}}$ is:

$$\mathcal{B}_{\mathcal{A}} = \{U_f \times U_p \mid U_f \subset \mathcal{H}_{\mathcal{F}}, U_p \subset \mathcal{H}_p\} \tag{5}$$

The topology for $\mathcal{A}$ is:

$$\tau_{\mathcal{A}} = \{\bigcup A \mid A \subseteq \mathcal{B}_{\mathcal{A}}\} \tag{6}$$

If only the sets of audible frequencies and pressures are considered, then the discretized acoustic space is:

$$\mathcal{A} = \mathcal{F} \times \mathcal{P} \tag{7}$$

with the discrete topology.

Neural Space

The neural space $S_{\mathcal{X}}$ is constructed in a similar fashion as $\mathcal{F}$ and $\mathcal{P}$, though the topology is slightly different. The idea is to partition $S_{\mathcal{X}}$ into subintervals that represent neurons and then to combine the subintervals contiguously to form synaptic intervals.

The neural space $S_{\mathcal{X}} \subset \mathbb{R}^+$ is a half-open interval representing the one dimensional tonotopic axis: $S_{\mathcal{X}} = [x_{min}, x_{max})$. $S_{\mathcal{X}}$ is partitioned into N_{cell} half-open intervals, each of width Δx and expressed as $[x_\alpha, x_\beta), x_\beta > x_\alpha$ or $[x_\alpha, x_\alpha + \Delta x)$. Each interval represents the length (Δx) of a single cell on the tonotopic axis. The set of intervals is expressed as:

$$\begin{aligned} \mathcal{H}_{x,1} &= \{h_{x_i,1} = [x_i, x_i + \Delta x)) \mid x_i \in S_{\mathcal{X}}, x_i \leq |S_{\mathcal{X}}| - \Delta x\} \\ &= \{h_{x,1} = [x_{min} + i\Delta x, x_{min} + (i+1)\Delta x) \mid i \in \mathbb{N}_0, i < N_{cell}\} \end{aligned} \tag{8}$$

The set $\mathcal{H}_{x,1}$ is a partition, which effectively discretizes $S_{\mathcal{X}}$ (see section above for a similar treatment). Each interval is uniquely identified by the point at the closed end (x_i in eq. 8). The set $\mathcal{X}$ containing these points is:

$$\begin{aligned} \mathcal{X} &= \{x_i \mid x_i = x_{min} + i\Delta x \mid x_i \in S_{\mathcal{X}}, 0 < i < N_{cell}\} \\ &= \{x_0, x_1, \ldots, x_{N_{cell}-1}\} \end{aligned} \tag{9}$$

A synaptic interval is also a half-open interval with length λ expressed as:

$$h_{x,\lambda} = [x, x + \lambda),\ x \in \mathcal{X}, \lambda \in S_\Lambda$$

where $S_\Lambda = [\lambda_{\min}, \lambda_{\max})$, $\lambda_{min} > 0, \lambda_{max} < |S_{\mathcal{X}}|$ is the range of values that the length can take. The length of the synaptic interval is defined to be a contiguous set of cells so that $h_{x,\lambda}$ is an integral multiple of cell length Δx. Letting $n_\lambda \in \mathbb{N}^+$ be the number of cells in the interval, the intervals may be re-expressed as:

$$h_{x,\lambda} = [x, x + \lambda),\ x \in \mathcal{X}, \lambda = n_\lambda \Delta x, n_\lambda \leq n_{\lambda,max} \leq N_{cells} \tag{10}$$

where $n_{\lambda,max}$ is the maximum number of cells in the interval. The set containing all possible interval lengths is :

$$\begin{aligned} \Lambda &= \{\lambda_{n_\lambda} \mid \lambda_{n_\lambda} = n\Delta x, n_\lambda \leq n_{\lambda,max} \leq N_{cell}\} \subset S_\Lambda \\ &= \{\lambda_1, \lambda_2, \ldots, \lambda_{max}\} \end{aligned} \tag{11}$$

As shown in the next section, sound pressure will be encoded as the length of the intervals. In order to ensure a full representation of sound pressure, a 'buffer' of $N_{cell} - n_{\max}$ cells is needed. Without the buffer, the maximum value of last interval is 1 cell. The set of identifying points for synaptic intervals is then:

$$\mathcal{X}_\lambda = \{x_1, x_2, \ldots, x_{N_\lambda}\} \subset \mathcal{X}; N_\lambda = N_{cell} - n_{max} \tag{12}$$

The set of synaptic intervals is expressed as:

$$\mathcal{H}_{x,\lambda} = \{h_{x,\lambda} = [x, x+\lambda) \mid x \in \mathcal{X}, \lambda \in \Lambda\} \tag{13}$$

The topology of $S_\mathcal{X}$ generated by the elements of $\mathcal{H}_{x,\lambda}$ is:

$$\tau_\mathcal{X} = \{\bigcup H_s \mid H_s \subseteq \mathcal{H}_{x,\lambda}\} \tag{14}$$

Mapping from acoustic space to neural space

The aim is to construct a mapping between the acoustic and neural spaces in such a way that allows for both encoding and decoding sounds in neural space.

Note that a pure tone $a_{f,p}$ corresponds to the ordered pair $(f,p) \in S_\mathcal{F} \times S_\mathcal{P}$ and an interval $h_{x,\lambda} = [x,x+\lambda)$ corresponds to the ordered pair $(x,\lambda) \in S_\mathcal{X} \times S_\Lambda$. The mapping (ψ) from acoustic to neural space is obtained by first defining mappings from frequency space $(S_\mathcal{F})$ to neural space $(S_\mathcal{X})$ and from pressure space $(S_\mathcal{P})$ to interval length space (S_Λ):

$$\begin{aligned} &\psi_f : S_\mathcal{F} \to \mathcal{X}, \psi_f(f) = x; \\ &\psi_p : S_\mathcal{P} \to S_\Lambda, \psi_p(p) = \lambda; \\ &\psi : S_\mathcal{F} \times S_\mathcal{P} \to S_\mathcal{X} \times S_\Lambda; \psi(f,p) = (\psi_f(f), \psi_p(p)) = (x,\lambda) \end{aligned} \tag{15}$$

By construction, the mappings are homeomorphisms.

After partitioning, the spaces are effectively discretized into $\mathcal{F} \subset S_\mathcal{F}, \mathcal{P} \subset S_\mathcal{P}, \mathcal{X}_\lambda \subset S_\mathcal{X}, \Lambda \subset S_\Lambda$. These are the functionally and biological relevant sets as they contain the audible frequencies and pressures that can be mapped into the compartmentalized neural space. Therefore, the mapping can be restricted to these sets:

$$\begin{aligned} &\psi_f\restriction_\mathcal{F} : \mathcal{F} \to \mathcal{X}_\lambda, \psi_f\restriction_\mathcal{F}(f) = x; \\ &\psi_p\restriction_\mathcal{P} : \mathcal{P} \to \lambda, \psi_p\restriction_\mathcal{P}(p) = \lambda; \\ &\psi\restriction_{\mathcal{F},\mathcal{P}} : \mathcal{F} \times \mathcal{P} \to \mathcal{X} \times \Lambda; \psi\restriction_{\mathcal{F},\mathcal{P}}(f,p) \\ &= (\psi_f\restriction_\mathcal{F}(f), \psi_p\restriction_\mathcal{P}(p)) = (x,\lambda) \end{aligned} \tag{16}$$

The maps are bijective if $|\mathcal{F}| = |\mathcal{X}_\lambda|$ and $|\mathcal{P}| = |\Lambda|$ and continuous because the restricted spaces have the discrete topology.

Algebraic operations

In the following, addition and multiplication operations for combining elements in acoustic and neural spaces are defined.

Operations in acoustic space

Complex sounds are composed of multiple pure tones of varying frequencies and intensities. The analyses will be limited to sets of audible frequencies ($\mathcal{F}$) and pressures ($\mathcal{P}$). Pure tones are combined with an addition ("+") operation defined as the 'union'.

$$+ : \mathcal{A} \times \mathcal{A} \to \mathcal{A}; a_{f_\alpha,p_\alpha} + a_{f_\beta,p_\beta} \stackrel{\text{def}}{=} a_{f_\alpha,p_\alpha} \cup a_{f_\beta,p_\beta} \tag{17}$$

One property that is potentially problematic is that the addition operation can produce a sound with the same frequency but different pressures, which is physically impossible (e.g. $a_{f_\alpha,p_\gamma} \cup a_{f_\alpha,p_\delta} = \{a_{f_\alpha,p_\gamma}, a_{f_\alpha,p_\delta}\}$). This may actually be a desirable property because the sound information may propagate through different channels in the auditory pathway before converging to a neural space (e.g. binaural stimuli). Nevertheless, assigning multiple pressure values to a single frequency may be avoided as follows. For $a_{f_\alpha,p_\alpha}, a_{f_\beta,p_\beta} \in \mathcal{A}$,

$$a_{f_\alpha,p_\alpha} + a_{f_\beta,p_\beta} = \begin{cases} \{a_{f_\alpha,p_\alpha}, a_{f_\beta,p_\beta}\}, & f_\alpha \neq f_\beta \\ a_{f,p_\gamma},\ p_\gamma = \max(p_\alpha, p_\beta), & f_\alpha = f_\beta \end{cases} \tag{18}$$

Operations in Neural Space

In neural space, addition ("+") is also defined as the union. For $h_{x_\alpha\lambda_\alpha}, h_{x_\beta\lambda_\beta} \in (S_\mathcal{X}, \tau_\mathcal{X})$

$$\begin{aligned} &+ : (S_\mathcal{X}, \tau_\mathcal{X}) \times (S_\mathcal{X}, \tau_\mathcal{X}) \to (S_\mathcal{X}, \tau_\mathcal{X}); \\ &h_{x_\alpha\lambda_\alpha} + h_{x_\beta\lambda_\beta} \stackrel{\text{def}}{=} h_{x_\alpha\lambda_\alpha} \cup h_{x_\beta\lambda_\beta} \end{aligned} \tag{19}$$

Generally, for any two synaptic intervals $(h_{x\lambda_\alpha}, h_{x\lambda_\beta})$, the addition operation yields two possibilities:

$$h_{x_\alpha\lambda_\alpha} + h_{x_\beta\lambda_\beta} = \begin{cases} h_{x\lambda}, x = \min(x_\alpha, x_\beta), \lambda = |h_{x\lambda_\alpha} \cup h_{x\lambda_\beta}|, & h_{x\lambda_\alpha} \cap h_{x\lambda_\beta} \neq \emptyset \\ \{h_{x_\alpha\lambda_\alpha}, h_{x_\beta\lambda_\beta}\}, & h_{x\lambda_\alpha} \cap h_{x\lambda_\beta} = \emptyset \end{cases} \tag{20}$$

For more than 2 synaptic intervals, the total length λ is given by the Inclusion-Exclusion principle.

The algebraic structure on $(S_\mathcal{X}, \tau_\mathcal{X})$ with the addition operation is a monoid since it inherits the algebraic properties of the union operation. In particular, addition is closed because the result is either a longer, half-open interval or two disjoint half-open intervals, either of which is an element of $\tau_\mathcal{X}$. Addition is commutative, associative, has the empty set as the identity element, and does not have an inverse.

Multiplication "$\cdot$" of synaptic intervals is defined as the set minus operation ($\setminus$). Given two intervals $h_{x_\alpha,\lambda_\alpha}, h_{x_\beta,\lambda_\beta} \in (S_\mathcal{X}, \tau_\mathcal{X})$ where $h_{x_\alpha,\lambda_\alpha}$ is the multiplier and $h_{x_\beta,\lambda_\beta}$ is the multiplicand,

$$\begin{aligned} &\bullet : (S_\mathcal{X}, \tau_\mathcal{X}) \times (S_\mathcal{X}, \tau_\mathcal{X}) \to (S_\mathcal{X}, \tau_\mathcal{X}); \\ &h_{x_\alpha,\lambda_\alpha} \cdot h_{x_\beta,\lambda_\beta} \stackrel{\text{def}}{=} h_{x_\beta,\lambda_\beta} \setminus h_{x_\alpha,\lambda_\alpha} \end{aligned} \tag{21}$$

Letting $\hat{\lambda} = |h_{x_\beta,\lambda_\beta} \setminus h_{x_\alpha,\lambda_\alpha}|$, the possible results of multiplication are:

$$
\begin{aligned}
&h_{x_\alpha,\lambda_\alpha} \cdot h_{x_\beta,\lambda_\beta} = \\
&\quad \begin{cases}
1.\, h_{x_\beta,\lambda_\beta}, & h_{x_\alpha,\lambda_\alpha} \cap h_{x_\beta,\lambda_\beta} = \emptyset \\
2.\, [x_\beta, x_\beta + \hat{\lambda}), & h_{x_\alpha,\lambda_\alpha} \cap h_{x_\beta,\lambda_\beta} \neq \emptyset, x_\beta < x_\alpha, h_{x_\alpha,\lambda_\alpha} \not\subset h_{x_\beta,\lambda_\beta} \\
3.\, [x_\delta, x_\delta + \hat{\lambda}), & h_{x_\alpha,\lambda_\alpha} \cap h_{x_\beta,\lambda_\beta} \neq \emptyset, x_\beta \geq x_\alpha, h_{x_\beta,\lambda_\beta} \not\subset h_{x_\alpha,\lambda_\alpha} \\
\qquad x_\delta = x_\beta + (\lambda_\beta - \hat{\lambda}) & \\
4.\, \emptyset, & h_{x_\beta,\lambda_\beta} \subset h_{x_\alpha,\lambda_\alpha} \\
5.\, \{[x_\beta, x_\alpha), [x_\alpha + \lambda_\alpha, x_\beta + \lambda_\beta)\}, & h_{x_\alpha,\lambda_\alpha} \subset h_{x_\beta,\lambda_\beta}
\end{cases}
\end{aligned}
\tag{22}
$$

The algebraic structure on $(S_\mathcal{X}, \tau_X)$ with the multiplication operation is a magma, with properties inherited from the set minus operation. Multiplication is closed because the set minus operation yields an interval that is either the empty set or a half-open interval(s) with a minimum length(s) of Δx and maximum length of λ_{max}. In either case, the resulting interval is in $(S_\mathcal{X}, \tau_\mathcal{X})$. While the $\emptyset$ is a left identity element, there is no unique inverse element since the result is the $\emptyset$ whenever the length of multiplier is greater than or equal to that of the multiplicand. It is also neither commutative nor associative.

Proposition 0.0.1. The *multiplication* operation is left but not right distributive over addition.

Proof. **Left distributive**: Let $h_{x_\alpha,\lambda_\alpha}, h_{x_\beta,\lambda_\beta}, h_{x_\gamma,\lambda_\gamma} \in (S_\mathcal{X}, \tau_\mathcal{X})$

$$
\begin{aligned}
&= h_{x_\gamma,\lambda_\gamma} \cdot (h_{x_\alpha,\lambda_\alpha} + h_{x_\beta,\lambda_\beta}) \\
&= (h_{x_\alpha,\lambda_\alpha} \cup h_{x_\beta,\lambda_\beta}) \setminus h_{x_\gamma,\lambda_\gamma} \\
&= h^c_{x_\gamma,\lambda_\gamma} \cap (h_{x_\alpha,\lambda_\alpha} \cup h_{x_\beta,\lambda_\beta}), \text{ 'c' is complement} \\
&= (h^c_{x_\gamma,\lambda_\gamma} \cap h_{x_\alpha,\lambda_\alpha}) \cup (h^c_{x_\gamma,\lambda_\gamma} \cap h_{x_\beta,\lambda_\beta}) \\
&= h_{x_\alpha,\lambda_\alpha} \setminus h_{x_\gamma,\lambda_\gamma} \cup h_{x_\beta,\lambda_\beta} \setminus h_{x_\gamma,\lambda_\gamma} \\
&= h_{x_\gamma,\lambda_\gamma} \cdot h_{x_\alpha,\lambda_\alpha} + h_{x_\gamma,\lambda_\gamma} \cdot h_{x_\beta,\lambda_\beta}
\end{aligned}
$$

Not Right distributive:

$$
\begin{aligned}
&(h_{x_\alpha,\lambda_\alpha} + h_{x_\beta,\lambda_\beta}) \cdot h_{x_\gamma,\lambda_\gamma} \\
&= h_{x_\gamma,\lambda_\gamma} \setminus (h_{x_\alpha,\lambda_\alpha} \cup h_{x_\beta,\lambda_\beta}) \\
&= h_{x_\gamma,\lambda_\gamma} \cap (h_{x_\alpha,\lambda_\alpha} \cup h_{x_\beta,\lambda_\beta})^c \\
&= h_{x_\gamma,\lambda_\gamma} \cap (h^c_{x_\alpha,\lambda_\alpha} \cap h^c_{x_\beta,\lambda_\beta}), \text{from de Morgan's law} \\
&\neq h_{x_\alpha,\lambda_\alpha} \cdot h_{x_\gamma,\lambda_\gamma} + h_{x_\beta,\lambda_\beta} \cdot h_{x_\gamma,\lambda_\gamma}
\end{aligned}
$$

□

While not Right distributive, a notable property is that the effect of two multipliers acting on a single multiplicand is that the operation can be performed sequentially:

$$
\begin{aligned}
&h_{x_\gamma,\lambda_\gamma} \cap (h^c_{x_\alpha,\lambda_\alpha} \cap h^c_{x_\beta,\lambda_\beta}), \text{(from Proposition 0.0.1)} \\
&= (h_{x_\gamma,\lambda_\gamma} \cap h^c_{x_\alpha,\lambda_\alpha}) \cap h^c_{x_\beta,\lambda_\beta} = (h_{x_\gamma,\lambda_\gamma} \cap h^c_{x_\beta,\lambda_\beta}) \cap h^c_{x_\alpha,\lambda_\alpha} \\
&= (h_{x_\gamma,\lambda_\gamma} \setminus h_{x_\alpha,\lambda_\alpha}) \setminus h_{x_\beta,\lambda_\beta} = (h_{x_\gamma,\lambda_\gamma} \setminus h_{x_\beta,\lambda_\beta}) \setminus h_{x_\alpha,\lambda_\alpha} \\
&= h_{x_\beta,\lambda_\beta} \cdot (h_{x_\alpha,\lambda_\alpha} \cdot h_{x_\gamma,\lambda_\gamma}) = h_{x_\alpha,\lambda_\alpha} \cdot (h_{x_\beta,\lambda_\beta} \cdot h_{x_\gamma,\lambda_\gamma})
\end{aligned}
$$

Place code with columnar organization and population rate code

In the mathematical model, the 'functional' unit is an interval that can vary in size, depending on the sound intensity. The indistinct borders are consistent with topographical organization of afferents [19]. An alternative organization is with classical columns [17]. The definition of a column has evolved [50] but for illustrative purposes, columns are defined here as having distinct borders; the enclosed neurons have identical receptive fields and hence function as a single unit. In this scheme, the location of the active column encodes frequency. Because the column dimension is fixed, sound pressure will be encoded as the average number of neurons that become active during the stimulus.

The number ($|\mathcal{F}|$) of frequencies that can be encoded in neural space depends on the column dimension. The neural space is partitioned into N_{cell}, non-overlapping half-open intervals to represent neurons (see above). The columns are also non-overlapping half open intervals, consisting of a contiguous set of n_{cell} neurons. Thus, the number of columns N_{col} that can fit into the neural space is $N_{col} = N_{cell}/n_{col}$. To construct a bijective mapping between acoustic and neural space, the number of frequency elements must be equal to that in neural space, that is: $|\mathcal{F}| = N_{cell}/n_{col}$. Therefore, $|\mathcal{F}|$ is maximal when $n_{col} = 1$ and decreases hyperbolically thereafter.

The number of cells (n_{on}) in a column that becomes active during a stimulus is taken to be proportional to the stimulus intensity. Therefore, the number of levels that can be represented is limited by the number of cells in each column. Hence, for bijective mapping from pressure ($\mathcal{P}$) to cells in the columns, $|\mathcal{P}| = n_{col}$, which is inverse of the condition for maximizing $|\mathcal{F}|$. This means that the increasing the number of frequency levels comes at the expense of the number of pressure levels and vice-versa.

The one potential advantage of a columnar organization/population rate code is that sounds with multiple tonal components can be more accurately encoded. Unlike with overlapping intervals, the representation of frequency components in neural space remain separated because the columns are disjoint. Thus, there are no ambiguities when the sound is composed of tones with similar frequencies.

Experimental evidence

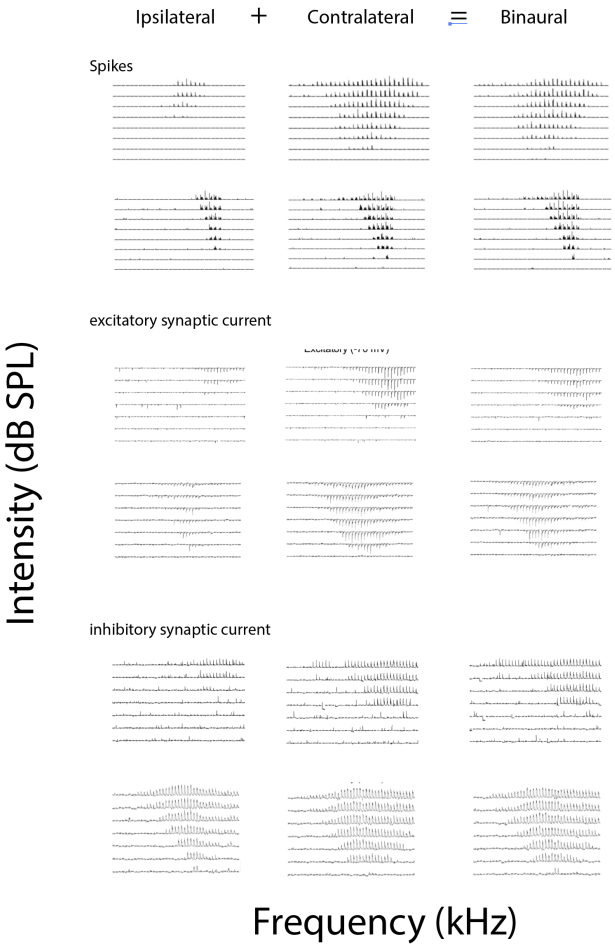

Experimental evidence for Addition operation Data adapted from reference [26]. Extracellular (top) and whole-cell voltage clamp (middle, bottom) recording from the central nucleus of the Inferior colliculus, which receives binaural inputs. The frequency response areas (FRA) were constructed by presenting pure tones of varying frequencies (abscissas) and intensities (ordinates) and documenting the responses. Tones were delivered ipsilaterally (left column), contralaterally (middle), and binaurally (right). As mentioned in the main text, the FRAs can be taken as an indicator of the spatial extent of synaptic field and activated area. The model predicts that because the contralateral response is greater than the ipsilateral response, the response evoked with binaural stimulation should equal that of contralateral stimulation. In all cases, the binaural FRAs was nearly identical to the contralateral FRAs. *Permission pending.*

References

[1] William M Siebert. "Frequency discrimination in the auditory system: Place or periodicity mechanisms?" In: *Proceedings of the IEEE* 58.5 (1970), pp. 723–730.

[2] Georg Von Bekesy and Ernest Glen Wever. *Experiments in hearing*. Vol. 8. McGraw-Hill New York, 1960.

[3] Jozef J Zwislocki and My Nguyen. "Place code for pitch: A necessary revision". In: *Acta oto-laryngologica* 119.2 (1999), pp. 140–145.

[4] Troy A Hackett et al. "Linking topography to tonotopy in the mouse auditory thalamocortical circuit". In: *Journal of Neuroscience* 31.8 (2011), pp. 2983–2995.

[5] Brian CJ Moore and Stephan MA Ernst. "Frequency difference limens at high frequencies: evidence for a transition from a temporal to a place code". In: *The Journal of the Acoustical Society of America* 132.3 (2012), pp. 1542–1547.

[6] Robert P Carlyon et al. "Pitch comparisons between electrical stimulation of a cochlear implant and acoustic stimuli presented to a normal-hearing contralateral ear". In: *Journal of the Association for Research in Otolaryngology* 11.4 (2010), pp. 625–640.

[7] Bertrand Delgutte. "Physiological models for basic auditory percepts". In: *Auditory computation*. Springer, 1996, pp. 157–220.

[8] JM Doughty and WR Garner. "Pitch characteristics of short tones. II. Pitch as a function of tonal duration." In: *Journal of Experimental Psychology* 38.4 (1948), p. 478.

[9] Brian CJ Moore. "Frequency difference limens for short-duration tones". In: *The Journal of the Acoustical Society of America* 54.3 (1973), pp. 610–619.

[10] Christophe Micheyl, Li Xiao, and Andrew J Oxenham. "Characterizing the dependence of pure-tone frequency difference limens on frequency, duration, and level". In: *Hearing Research* 292.1-2 (2012), pp. 1–13.

[11] Christophe Micheyl, Paul R Schrater, and Andrew J Oxenham. "Auditory frequency and intensity discrimination explained using a cortical population rate code". In: *PLoS computational biology* 9.11 (2013), e1003336.

[12] Brenda J Hefti and Philip H Smith. "Anatomy, Physiology, and Synaptic Responses of Rat Layer V Auditory Cortical Cells and Effects of Intracellular GABAABlockade". In: *Journal of Neurophysiology* 83.5 (2000), pp. 2626–2638.

[13] Anne-Marie M Oswald and Alex D Reyes. "Maturation of intrinsic and synaptic properties of layer 2/3 pyramidal neurons in mouse auditory cortex". In: *Journal of neurophysiology* 99.6 (2008), pp. 2998–3008.

[14] AD Reyes, EW Rubel, and WJ Spain. "Membrane properties underlying the firing of neurons in the avian cochlear nucleus". In: *Journal of Neuroscience* 14.9 (1994), pp. 5352–5364.

[15] Xiaoqin Wang et al. "Neural coding of temporal information in auditory thalamus and cortex". In: *Neuroscience* 154.1 (2008), pp. 294–303.

[16] Mounya Elhilali et al. "Dynamics of precise spike timing in primary auditory cortex". In: *Journal of Neuroscience* 24.5 (2004), pp. 1159–1172.

[17] Vernon B Mountcastle. "Modality and topographic properties of single neurons of cat's somatic sensory cortex". In: *Journal of neurophysiology* 20.4 (1957), pp. 408–434.

[18] David H Hubel and Torsten N Wiesel. "Receptive fields, binocular interaction and functional architecture in the cat's visual cortex". In: *The Journal of physiology* 160.1 (1962), pp. 106–154.

[19] Arnold L Towe. "Notes on the Hypothesis of Columnar Organization in Somatosensory Cerebral Cortex; pp. 32–47". In: *Brain, Behavior and Evolution* 11.1 (1975), pp. 32–47.

[20] Christoph E Schreiner. "Spatial distribution of responses to simple and complex sounds in the primary auditory cortex". In: *Audiology and Neurotology* 3.2-3 (1998), pp. 104–122.

[21] Tianying Ren, Wenxuan He, and David Kemp. "Reticular lamina and basilar membrane vibrations in living mouse cochleae". In: *Proceedings of the National Academy of Sciences* 113.35 (2016), pp. 9910–9915.

[22] Monita Chatterjee and Jozef J Zwislocki. "Cochlear mechanisms of frequency and intensity coding. I. The place code for pitch". In: *Hearing research* 111.1-2 (1997), pp. 65–75.

[23] William M Siebert et al. "Stimulus transformations in the peripheral auditory system". In: *Recognizing patterns* 104.133 (1968), pp. 602–615.

[24] Robert B Levy and Alex D Reyes. "Coexistence of lateral and co-tuned inhibitory configurations in cortical networks". In: *PLoS computational biology* 7.10 (2011), e1002161.

[25] Robert B Levy and Alex D Reyes. "Spatial profile of excitatory and inhibitory synaptic connectivity in mouse primary auditory cortex". In: *Journal of Neuroscience* 32.16 (2012), pp. 5609–5619.

[26] Xiaorui R Xiong et al. "Interaural level difference-dependent gain control and synaptic scaling underlying binaural computation". In: *Neuron* 79.4 (2013), pp. 738–753.

[27] Michael Epstein and Mary Florentine. "Binaural loudness summation for speech presented via earphones and loudspeaker with and without visual cues". In: *The Journal of the Acoustical Socient of America* 131 (2012), pp. 3981–3988.

[28] Alex Reyes et al. "Target-cell-specific facilitation and depression in neocortical circuits". In: *Nature neuroscience* 1.4 (1998), pp. 279–285.

[29] WR Thurlow and S Bernstein. "Simultaneous Two-Tone Pitch Discrimination". In: *The Journal of the Acoustical Society of America* 29.4 (1957), pp. 515–519.

[30] Willard R Thurlow and Irving L Rawlings. "Discrimination of number of simultaneously sounding tones". In: *The Journal of the Acoustical Society of America* 31.10 (1959), pp. 1332–1336.

[31] Christophe NJ Stoelinga and Robert A Lutfi. "Discrimination of the spectral density of multitone complexes". In: *The Journal of the Acoustical Society of America* 130.5 (2011), pp. 2882–2890.

[32] Bertram Scharf. "Complex sounds and critical bands." In: *Psychological Bulletin* 58.3 (1961), p. 205.

[33] Eberhard Zwicker, Georg Flottorp, and Stanley Smith Stevens. "Critical band width in loudness summation". In: *The Journal of the Acoustical Society of America* 29.5 (1957), pp. 548–557.

[34] Imme Stiebler and Gunter Ehret. "Inferior colliculus of the house mouse. I. A quantitative study of tonotopic organization, frequency representation, and tone-threshold distribution". In: *Journal of Comparative Neurology* 238.1 (1985), pp. 65–76.

[35] Feng Luo et al. "Three-dimensional tonotopic organization of the C57 mouse cochlear nucleus". In: *Hearing research* 257.1-2 (2009), pp. 75–82.

[36] I Stiebler et al. "The auditory cortex of the house mouse: left-right differences, tonotopic organization and quantitative analysis of frequency representation". In: *Journal of Comparative Physiology A* 181.6 (1997), pp. 559–571.

[37] Wei Guo et al. "Robustness of cortical topography across fields, laminae, anesthetic states, and neurophysiological signal types". In: *Journal of Neuroscience* 32.27 (2012), pp. 9159–9172.

[38] John B Issa et al. "Multiscale optical Ca2+ imaging of tonal organization in mouse auditory cortex". In: *Neuron* 83.4 (2014), pp. 944–959.

[39] Daniel E Winkowski and Patrick O Kanold. "Laminar transformation of frequency organization in auditory cortex". In: *Journal of Neuroscience* 33.4 (2013), pp. 1498–1508.

[40] Gideon Rothschild, Israel Nelken, and Adi Mizrahi. "Functional organization and population dynamics in the mouse primary auditory cortex". In: *Nature neuroscience* 13.3 (2010), p. 353.

[41] Sharba Bandyopadhyay, Shihab A Shamma, and Patrick O Kanold. "Dichotomy of functional organization in the mouse auditory cortex". In: *Nature neuroscience* 13.3 (2010), p. 361.

[42] JJ Zwislocki. "What is the cochlear place code for pitch?" In: *Acta oto-laryngologica* 111.2 (1991), pp. 256–262.

[43] ML Sutter et al. "Organization of inhibitory frequency receptive fields in cat primary auditory cortex". In: *Journal of Neurophysiology* 82.5 (1999), pp. 2358–2371.

[44] Rishidev Chaudhuri and Ila Fiete. "Computational principles of memory". In: *Nature neuroscience* 19.3 (2016), p. 394.

[45] Jeremie Barral, Xiao-Jing Wang, and Alex D Reyes. "Propagation of temporal and rate signals in cultured multilayer networks". In: *Nature communications* 10.1 (2019), pp. 1–14.

[46] Jian Wang, Donald Caspary, and Richard J Salvi. "GABA-A antagonist causes dramatic expansion of tuning in primary auditory cortex". In: *Neuroreport* 11.5 (2000), pp. 1137–1140.

[47] Fiona EN LeBeau, Manuel S Malmierca, and Adrian Rees. "Iontophoresis in vivo demonstrates a key role for GABAA and glycinergic inhibition in shaping frequency response areas in the inferior colliculus of guinea pig". In: *Journal of Neuroscience* 21.18 (2001), pp. 7303–7312.

[48] Carina Curto et al. "Combinatorial neural codes from a mathematical coding theory perspective". In: *Neural computation* 25.7 (2013), pp. 1891–1925.

[49] Leslie C Osborne et al. "The neural basis for combinatorial coding in a cortical population response". In: *Journal of Neuroscience* 28.50 (2008), pp. 13522–13531.

[50] Jonathan C Horton and Daniel L Adams. "The cortical column: a structure without a function". In: *Philosophical Transactions of the Royal Society B: Biological Sciences* 360.1456 (2005), pp. 837–862.